Shape Analysis of the Corpus Callosum and Cerebellum in Female MS Patients with Different Clinical Phenotypes

DENIZ SIGIRLI,[1]* ILKER ERCAN,[1] SENEM TURAN OZDEMIR,[2] OZLEM TASKAPILIOGLU,[3] BAHATTIN HAKYEMEZ,[4] AND OMER FARUK TURAN[3]

[1]Department of Biostatistics, Faculty of Medicine, Uludag University, Bursa, Turkey
[2]Department of Anatomy, Faculty of Medicine, Uludag University, Bursa, Turkey
[3]Department of Norology, Faculty of Medicine, Uludag University, Bursa, Turkey
[4]Department of Radiology, Faculty of Medicine, Uludag University, Bursa, Turkey

ABSTRACT

The aim of this study was to investigate the shape differences in the corpus callosum (CC) and cerebellum of female relapsing-remitting multiple sclerosis (RRMS) and secondary progressive multiple sclerosis (SPMS) patients compared with healthy controls. This study was conducted using the magnetic resonance imaging scans of 15 control subjects, 26 RRMS, and 14 SPMS patients. The data obtained from the landmark coordinates were analyzed with statistical shape analysis. The landmarks that were chosen to determine the shape differences of the CC and cerebellum have been identified and used in previous studies. In addition to these landmarks, constructed landmarks were determined and used to assess regional shape differences better. The shapes of the CC and cerebellum showed statistically significant differences from the controls when compared with both the RRMS and SPMS patients. It was found that the deformation observed from controls to SPMS was greater than the deformation from controls to RRMS, both for the CC and cerebellum. In conclusion, this study revealed CC and cerebellar shape change in RRMS and SPMS, and showed that deformations both in CC and cerebellum advances with the disease progression. Anat Rec, 295:1202–1211, 2012.

Key words: multiple sclerosis; corpus callosum; cerebellum; statistical shape analysis; geometric morphometrics

INTRODUCTION

Multiple sclerosis (MS) is a frequently chronic, disabling, inflammatory, and demyelinating disease of the central nervous system that disproportionately affects young adults and women. In majority of patients, it is characterized by relapses that results from disseminated focal (mostly periventricular in the supratentorial region), immune-mediated demyelination and is accompanied by variable axonal damage and loss, in addition to reactive gliosis. During the early phase of the disease, relapses may fully recover; however, after the relapsing-remitting phase, the secondary progression develops (Confavreux and Vukusic, 2006; Compston and Coles, 2008). Although it is traditionally thought that MS is more closely associated with white matter (WM) than with gray matter (GM) atrophy, recent studies have confirmed that cortical GM pathology and diffuse WM and GM changes can play a major role in the secondary progression of MS (Quarantelli et al., 2003; Morgen et al., 2006; Anderson et al., 2009; Reynolds et al., 2011).

Neurological disease can cause atrophy of the part of the brain resulting in a change in its size and shape.

*Correspondence to: Deniz Sigirli, PhD; Department of Biostatistics, Uludag University, Gorukle Campus, 16059, Bursa, Turkey. E-mail: sigirli@uludag.edu.tr

Received 19 December 2011; Accepted 9 April 2012.

DOI 10.1002/ar.22493
Published online 14 May 2012 in Wiley Online Library (wileyonlinelibrary.com).

TABLE 1. Demographic and clinical details of MS patients and controls

		Controls ($n = 15$)	Relapsing remitting MS ($n = 26$)	Secondary progressive MS ($n = 14$)	P-value
Age, years (mean ± SD)		37.000 ± 10.935	33.731 ± 8.087	41.000 ± 8.357	0.058
Disease duration, months (median (min-max))		–	39 (8–204)	141 (48–204)	0.001
EDSS	≤ 2.5 (n, %)	–	14 (53.846)	5 (35.714)	0.445
	> 2.5 (n, %)	–	12 (46.154)	9 (64.286)	
Lesion in the brainstem and/or cerebellum	+(n, %)	–	13 (50)	10 (71.429)	0.331
	−(n, %)	–	13 (50)	4 (28.571	

SD: Standard deviation, EDSS: Expanded Disability Status Scale.

Brain atrophy, a well-known feature of MS, can extensively affect both the WM and GM. The corpus callosum (CC) is the largest compact white matter fiber tract in the human brain and is involved in interhemispheric information transfer. During the disease course of MS, the CC is frequently damaged, and CC atrophy is a common manifestation observed in MS patients. Moreover, several recent studies have suggested that the cerebellar cortex may be an important locus of tissue damage in MS patients (Ceccarelli et al., 2008; Anderson et al., 2009; Ramasamy et al., 2009). These studies demonstrated significant atrophy in the volumes of the infratentorial structures, including the cerebellum, in MS patients. This atrophy may have resulted in a change, in the size and shape of the cerebellum in MS patients.

Statistical shape analysis has become an increasing interest to the neuroimaging community. Many different methods have been used to measure anatomical brain structures quantitatively. These studies are often based on global volume and area measurements, which are intuitive features that may provide insight into the progression of the atrophy or dilatation that is caused by the disease. However, the structural changes that occur at specific locations are not sufficiently reflected in these volume and area measurements. In addition, despite the presence of shape differences between the same organs of two different individuals, it is possible that these organs may have the same volume and area measurements. Most of the studies in medicine are related with the examination of geometrical properties of an organ or organism. Nowadays, an organ or organism's appearance or shape began to be used as input data by the development of the imaging techniques (Ercan et al., 2012). Statistical shape analysis compares body forms by using specific landmarks determined by anatomical prominences. In recent years, it has been widely used in biomedical field to study various structures of interest to identify morphometric abnormalities associated with a particular condition or disease assisting with diagnosis and treatment (Styner et al., 2004; Sonat et al., 2009; Wan et al., 2010; Colak et al., 2011; Ercan et al., 2012; Sibony et al., 2011; Weisbecker, 2011).

The aim of this study was to investigate the shape differences in the CC and cerebellum of female relapsing-remitting MS (RRMS) and secondary progressive MS (SPMS) patients compared with healthy controls. We used the statistical shape analysis to examine the shape changes of the CC and cerebellar morphology in two clinical MS subtypes. A configuration of the landmarks was identified in the brain magnetic resonance imaging (MRI) midsagittal sections. The landmarks that were chosen to determine the shape differences of the CC and cerebellum have been identified and used in previous studies (Tibbo et al., 1998; DeQuardo et al., 1999; Ozdemir et al., 2007; Weinberg, 2009). In addition to these landmarks, constructed landmarks were determined and used to assess regional shape differences better.

MATERIAL AND METHODS

Subjects

This study was conducted using the MRI scans of 15 control subjects [age: 37.0 ± 10.9 years (24–61); mean ± SD (min–max)], 26 RRMS patients [age: 33.7 ± 8.1 years (23–52)], and 14 SPMS patients [age: 41.0 ± 8.4 years (30–57)]. The median duration of the MS disease was 39 (8–204) months [median (min–max)] for the relapsing-remitting group and 141 months (48–204) for the secondary progressive group (Table 1).

The MRI scans of the female RRMS patients, SPMS patients and controls, admitted into the Department of Radiology, Faculty of Medicine, Uludag University between April 2009 and April 2010, were retrospectively included. All of the MS patients fulfilled the McDonald criteria (McDonald et al., 2001), were diagnosed with the "relapsing-remitting" and "secondary progressive" clinical forms, and are under clinical and radiological remission. The classification and scoring of the MS patients were determined by a trained neurologist. The SPMS was defined as the initial relapsing-remitting disease course followed by more than 12 months of a continuous worsening of neurological function ($\geq$0.5 EDSS-expanded disability status scale point) that could not be explained by the relapses. In addition, patients with neurological disorders, diabetes mellitus, hypertension, and so forth, were excluded from this study. All of the patients were treated in the Department of Neurology, Faculty of Medicine, at Uludag University. The patients were examined by an experienced neuroradiologist for the presence of infratentorial lesions. Moreover, the presence of an infratentorial lesion was defined as the presence of a brainstem and/or cerebellar lesion.

The institutional review board approved this retrospective study, and all of the participants gave their informed consent before beginning this study.

TABLE 2. A descriptive list of the landmarks used for the corpus callosum

Landmark	Landmark definition
1	Anterior most point of the CC
2	Interior notch of the splenium
3	Inferior tip of the splenium
4	Posterior-most point of the CC
5	Top most point of the splenium
6	Top most point of the CC
7	Posterior angle of the genu
8	Posterior tip of the genu
9	The point at which the line that passes through landmark 7, is perpendicular to the segment, which was drawn from landmark 1 to landmark 7, and cuts the upper bound of the CC. 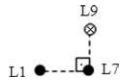
10	The point at which the line that passes through landmark 6, is perpendicular to the segment, which was drawn from landmark 5 to landmark 6, and cuts the lower bound of the CC. 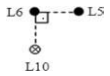
11	The point at which the line that passes through the midpoint of the segment, which was drawn from landmark 5 to landmark 6, is perpendicular to this segment, and cuts the upper bound of the CC. 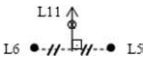
12	The point at which the line that passes through the midpoint of the segment, which was drawn from landmark 6 to landmark 9, is perpendicular to this segment, and cuts the lower bound of the CC. 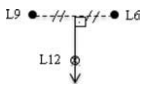
13	The point at which the line that passes through the midpoint of the segment, which was drawn from landmark 6 to landmark 9, is perpendicular to this segment, and cuts the upper bound of the CC. 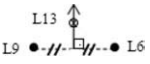
14	The point at which the line that passes through the midpoint of the segment, which was drawn from landmark 7 to landmark 12, is perpendicular to this segment, and cuts the lower bound of the CC. 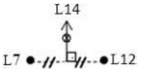
15	The point at which the line that passes through landmark 7 and the midpoint of the segment, which was drawn from landmark 1 to landmark 8, and cuts the left boundary of the CC. 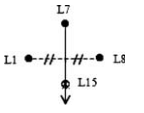
16	The point at which the line that passes through landmark 11 and the midpoint of the segment, which was drawn from landmark 2 to landmark 10, and cuts the lower bound of the CC. 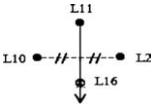

CC: corpus callosum.

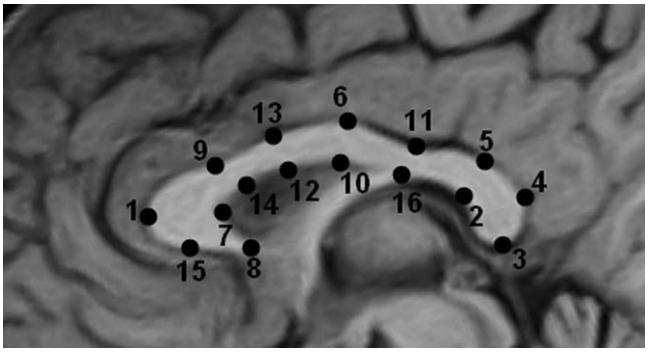

Fig. 1. T1-weighted midsagittal slice demonstrating the CC landmarks.

TABLE 3. A descriptive list of the landmarks used for the cerebellum

Landmark	Landmark definition
1	Velum medullare superius angulation-cerebellar outline junction
2	Superior cerebellum
3	Primary fissure-cerebellar outline junction
4	Posterior cerebellum
5	Prepyramidal fissure-cerebellar outline junction
6	Inferior cerebellum
7	Velum medullare inferius angulation-cerebellar outline junction
8	Fastigium cerebelli

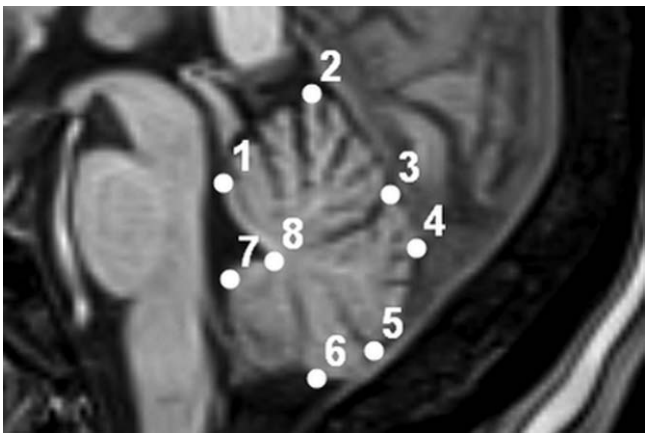

Fig. 2. T1-weighted midsagittal slice demonstrating the cerebellar landmarks.

MRI Examinations

MRIs were performed in a 1.5-Tesla Magnet (Magnetom Vision Plus, Siemens Medical Solutions, Erlangen, Germany) with a standard head coil. The images were acquired using a three-dimensional magnetization prepared-rapid acquisition gradient echo (3D MP-RAGE) sequences with the following parameters: TR/TE/TI/flip angle = 10/4/300/10-degree angle, 250 FOV, 1.25 mm

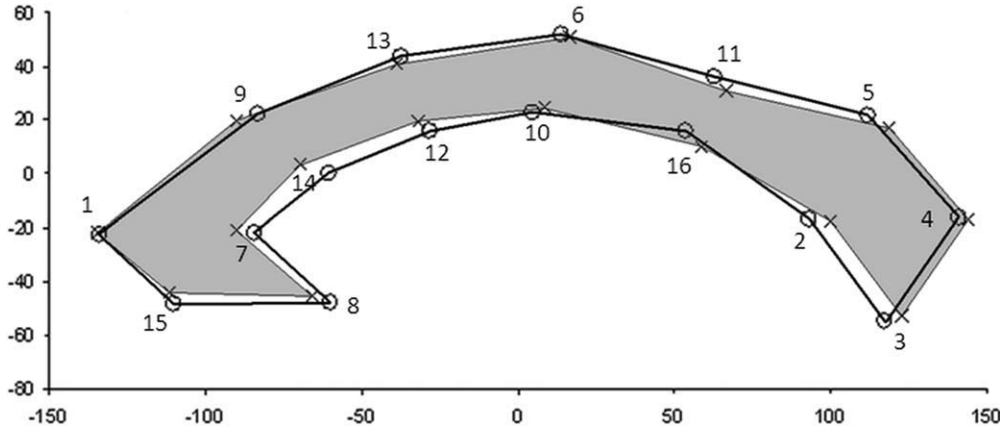

Fig. 3. Procrustes mean shapes for the CC images of relapsing-remitting MS patients and controls (Cases: x, Controls: o).

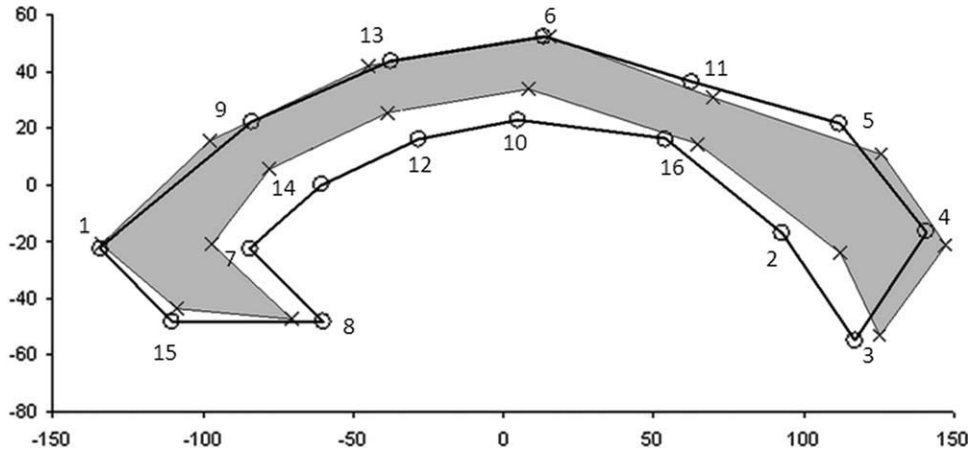

Fig. 4. Procrustes mean shapes for the corpus callosum (CC) images of secondary progressive MS patients and Controls (Cases: x, Controls: o).

slice, 192 × 256 matrix, 1 Nex. Furthermore, the sequences were chosen to provide good gray matter- and white matter-contrast. The scanner alignment tool and immobilization of the head helped to ensure the patient's standardized position.

Collection of Two-Dimensional Landmarks

The midsagittal section that most clearly displayed the cerebral aqueduct, CC and superior colliculus was manually selected from each of the sagittal planes. The anterior to posterior commissure line and interhemispheric fissure were identified and used to align the brains of all of the subjects at a standard position. We implemented a statistical shape analysis by using homologous anatomical landmarks, which were selected as the most relevant. Eight anatomical landmarks on the CC were defined as in Ozdemir et al. (2007). To better describe the shape of the brain structure, 8 more landmarks were constructed by referencing these anatomical landmarks. A descriptive list of these 16 chosen landmarks for the CC is shown in Table 2. Landmarks used for CC are demonstrated on MRI image of a control subject (Fig. 1).

Eight midline cerebellar landmarks were selected from the image corresponding to the midsagittal plane. The landmarks were chosen based on reliability, maximizing anatomical coverage, and cerebellar morphological descriptions. The cerebellum has traditionally been recognized as having three anterior-posterior divisions: the anterior lobe (lobules I-V) is separated from the posterior lobe by the primary fissure, and the posterior lobe (lobules V-IX) is separated from the flocculonodular lobe (lobule X) by the posterolateral fissure (Stoodley and Schmahmann, 2010). In another study, Pierson et al. (2002) have divided the cerebellar cortex into three sections as anterior lobe (lobules I-V), superior-posterior lobe (lobule VI and crus I of VIIA), and inferior posterior lobe (crus II of VIIA, VIIB, VIII, IX, and X). The names and boundaries of the lobes that have been assigned by Pierson et al. (2002) were used for the cerebellum in our study. Besides, only anterior lobe (covered by the landmark 1, 2, 3, and 8) and posterior lobe (covered by landmark 3, 4, 5, 6, 7, and 8), which are separated by the

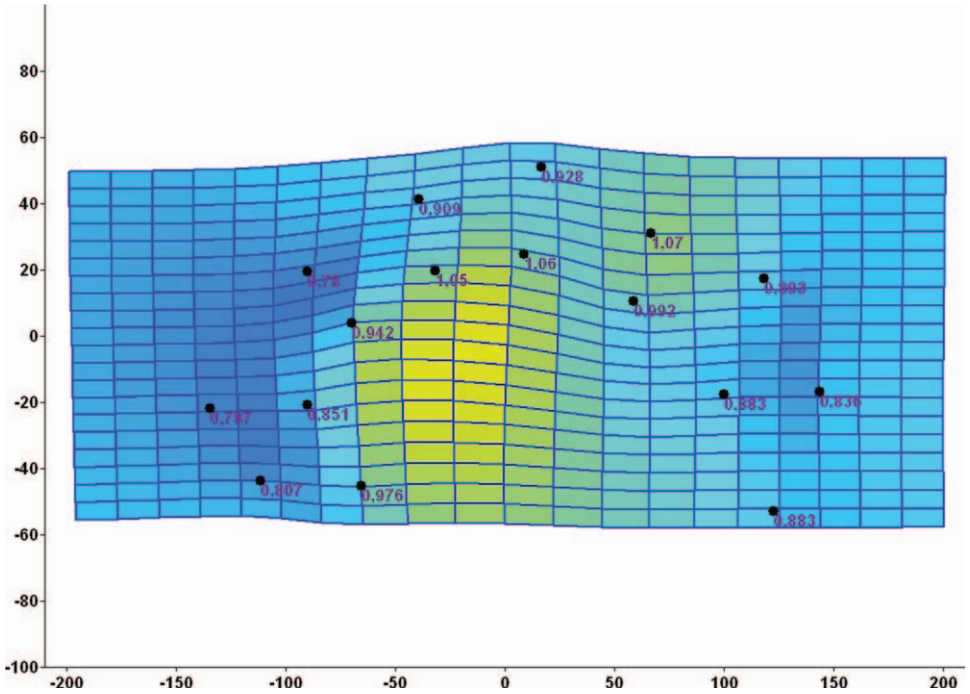

Fig. 5. A thin-plate spline demonstrating the average CC shape deformation from controls to relapsing-remitting MS patients.

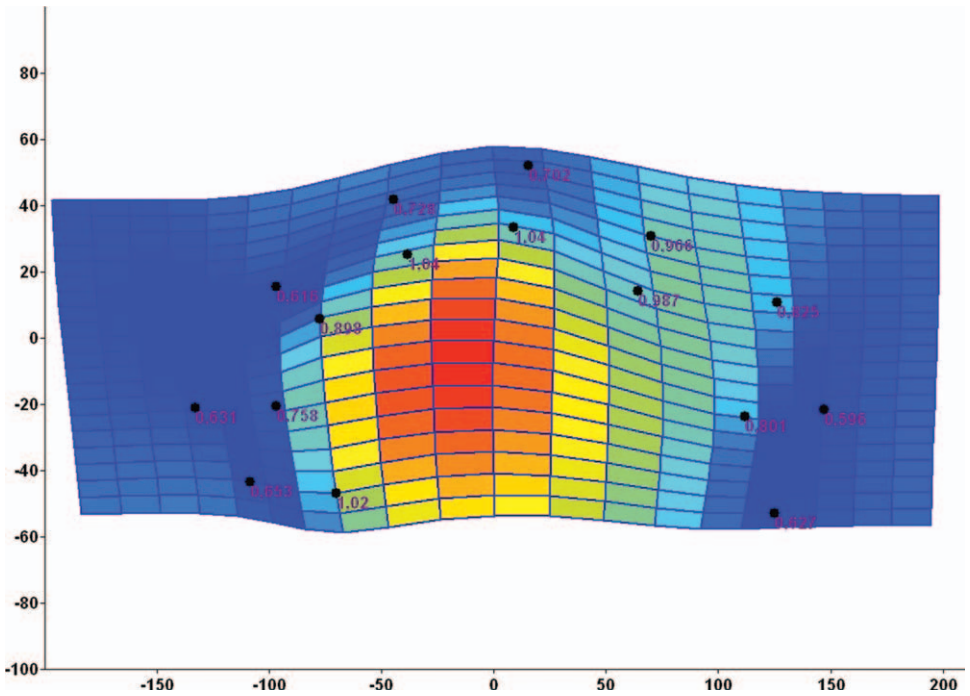

Fig. 6. A thin-plate spline demonstrating the average CC shape deformation from controls to secondary progressive MS patients.

primary fissure, were evaluated in the midsagittal MRI images because we did not identified the horizontal fissure as a landmark. A descriptive list of these anatomical landmarks is shown in Table 3. Landmarks used for cerebellum are demonstrated on MRI image of a control subject (Fig. 2).

The selected landmarks were marked on the digital images by using the TPSDIG 2.16 software (Rohlf,

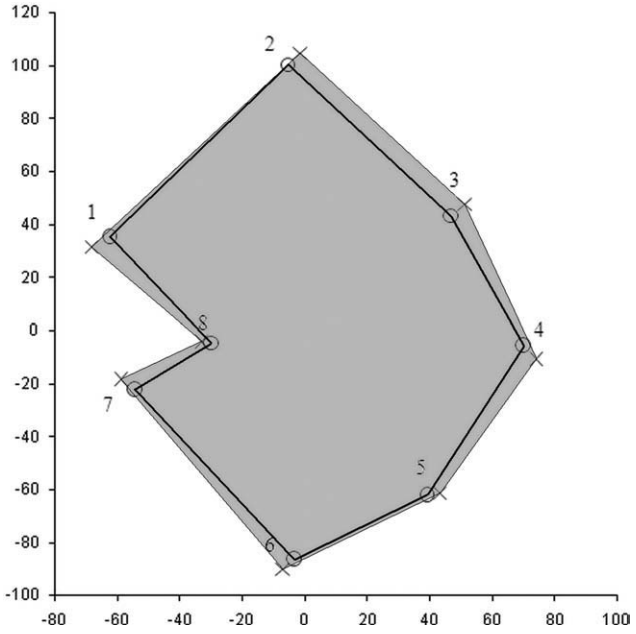

Fig. 7. Procrustes mean shapes for cerebellum images of relapsing remitting MS patients and controls (Cases: x, Controls: o).

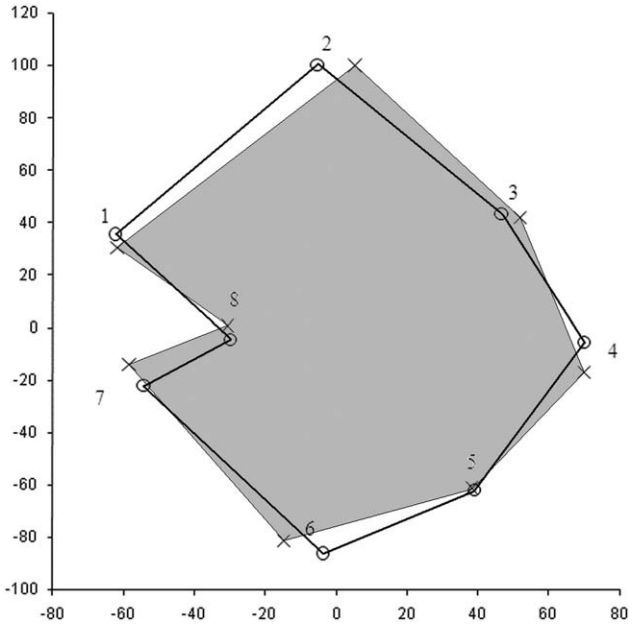

Fig. 8. The Procrustes mean shapes for cerebellar images of secondary progressive MS patients and controls (Cases: x, Controls: o).

2010). All of the points of these landmarks fell within the criteria outlined by Bookstein (1991) and included extreme points, terminals, and maxima of curvature, as well as other local shape processes.

Statistical Analysis

A generalized Procrustes analysis was used to evaluate the shapes. The homogeneity of the variance–covariance matrices was examined using the Box-M test (Dryden and Mardia, 1998). Because the variance–covariance matrices were not homogeneous ($P < 0.001$), the James F_J test was used to compare the shapes of the CC between the control and relapsing-remitting MS group, between the control and secondary progressive MS group. Similarly, this test was also used to compare the shapes of the cerebellum between the control and secondary progressive MS group. The Hotelling T^2 test was used to compare the shapes of the cerebellum between the control and relapsing-remitting MS group, and to compare the shapes of the CC and cerebellum between the lesion and nonlesion groups because the variance–covariance matrices were homogeneous ($P = 0.555$, $P = 0.323$ and $P = 0.144$, respectively) (Dryden, 2009).

The Procrustes mean shapes were computed and the shape deformations of the CC and cerebellum were evaluated using a thin plate spline (TPS) analysis. In accordance with the TPS analysis, the points exhibiting the greatest enlargements or reductions were labeled as deformations.

The ANOVA, Mann-Whitney U test, and Chi-square tests were performed to compare the demographic data between the groups.

Shapes 1.1-3 package from the R 2.12.1 software with an open-source code was used for the statistical shape analysis (Dryden, 2009). PAST version 2.04 was used for TPS analysis (Hammer et al., 2001). SPSS 16.0 for Windows was used for basic statistical tests.

Landmark Reliability

We calculated the intrarater reliability coefficient for a two-facet crossed design (landmark pairs-by-rater-by subject) based on the generalizability theory (GT) (Ercan et al., 2008). In the GT, the reliability for the relative (norm referenced) interpretations is referred to as the generalizability coefficient (Dimitrov, 2006). In this study, a single rater marked the anatomical landmarks. The reliability of the rater was judged using repeated landmarks on groups. Landmarks on CC and cerebellum were collected by a single investigator, and after a month, the same investigator re-marked these same landmarks on all of the images again. The analysis indicated good repeatability for CC and cerebellum ($G = 0.9988$ and $G = 0.9966$, respectively).

RESULTS

Although there was no statistically significant difference found between the groups in terms of age, EDDS score (<2.5 vs. ≥ 2.5) and lesion presence, there was a significant difference observed between the patient groups in terms of disease duration, which was expected (Table 1).

Corpus Callosum (CC)

There was no statistical significance between the lesion and nonlesion groups in terms of the CC shape ($P = 0.642$). The CC shape of controls was significantly different from the CC shape of the relapsing-remitting and secondary progressive patients ($P < 0.001$ and $P < 0.001$, respectively) (Figs. 3 and 4).

Furthermore, shape deformations were observed from controls to RRMS patients (Fig. 5). The maximum

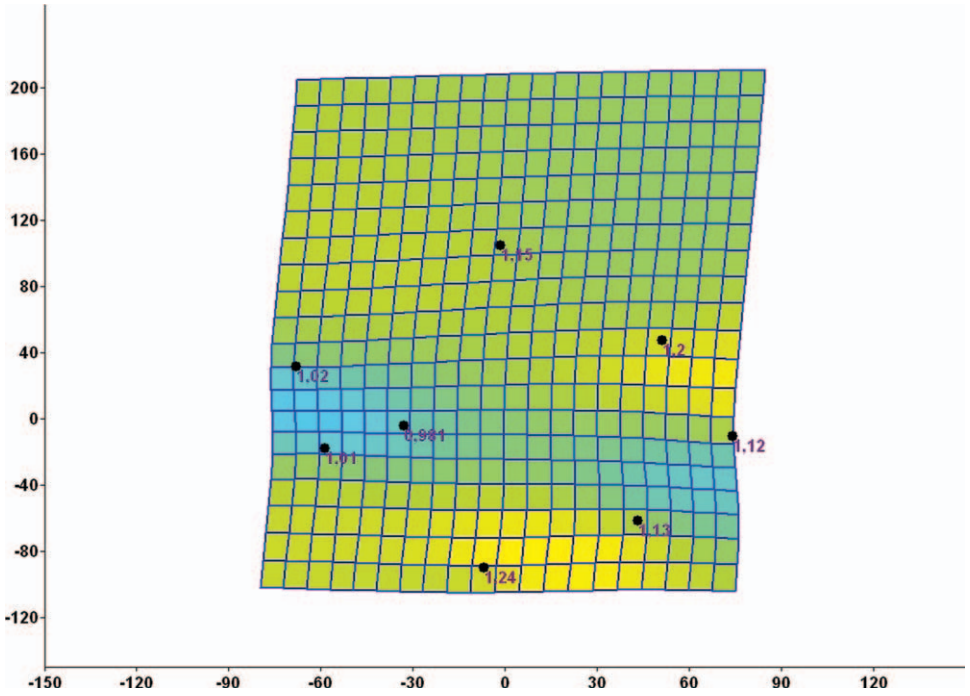

Fig. 9. A thin-plate spline demonstrating the average cerebellar shape deformation from controls to relapsing-remiting MS patients.

deformations were determined to be located in the anterior region of the CC. Shape deformations were also observed from controls to SPMS patients, and it is found that the maximum deformations were localized to the anterior region and trunk of the CC (Fig. 6). In addition, the CC shape deformation from controls to SPMS patients was greater than the deformations observed from controls to RRMS patients.

Cerebellum

There was no statistical significance between the lesion and nonlesion groups in terms of the cerebellar shape ($P = 0.832$). A significant difference was determined between the cerebellar shape of RRMS patients and controls ($P = 0.005$), as well as between SPMS patients and controls ($P < 0.001$) (Figs. 7 and 8).

In the relapsing-remitting group, the maximum deformations were particularly localized in the region of the posterior lobe of the cerebellum (especially in landmarks 3, 4, 5, and 6). Moreover, limited deformations were identified in the region of anterior lobe of the cerebellum (especially in landmark 2). In the secondary progressive group, the maximum deformations were identified in the anterior lobe of the cerebellum (especially in landmarks 1 and 8), and fewer deformations were found in the region of the inferior posterior lobe (especially in landmark 6). The cerebellar shape deformation from the controls to the secondary progressive MS patients was greater than the deformation from the controls to the relapsing-remitting MS patients (Figs. 9 and 10).

DISCUSSION

We performed statistical shape analysis of the changes in the shapes of CC and cerebellum in MS patients. In this study, we used a landmark-based shape analysis approach and focused on the female MS patients and controls. Since gender is an important factor that influences the size and shape of the human brain, only females were involved in this study to construct a homogeneous study sample. We have shown that the CC shape of controls was significantly different from the CC shape of the RRMS and SPMS patients. In addition, a significant difference was determined between the cerebellar shape of RRMS patients and controls, as well as between SPMS patients and controls. We found that maximum deformation was in the anterior region of the CC (genu and rostrum) in both clinical phenotypes of MS, being more prominent in SPMS. Additionally, there were deformations in the truncus of the CC in SPMS patients. Another important finding of this study was that deformation of cerebellum was more pronounced in SPMS than RRMS.

In this study, the CC was selected because it is the largest compact white matter-fiber bundle of the brain, which connects cortical and subcortical regions of the two hemispheres, thus allowing interhemispheric transfer of auditory, sensory, and motor information that is central for maintaining normal cognitive performance (Hines et al., 1992). CC atrophy which is observed in different disease groups such as MS, schizophrenia, Alzheimer's disease, autism and Behçet's disease, is frequently presented in global volume studies using different methods. But few studies have been performed on the regional differences in the CC using the shape

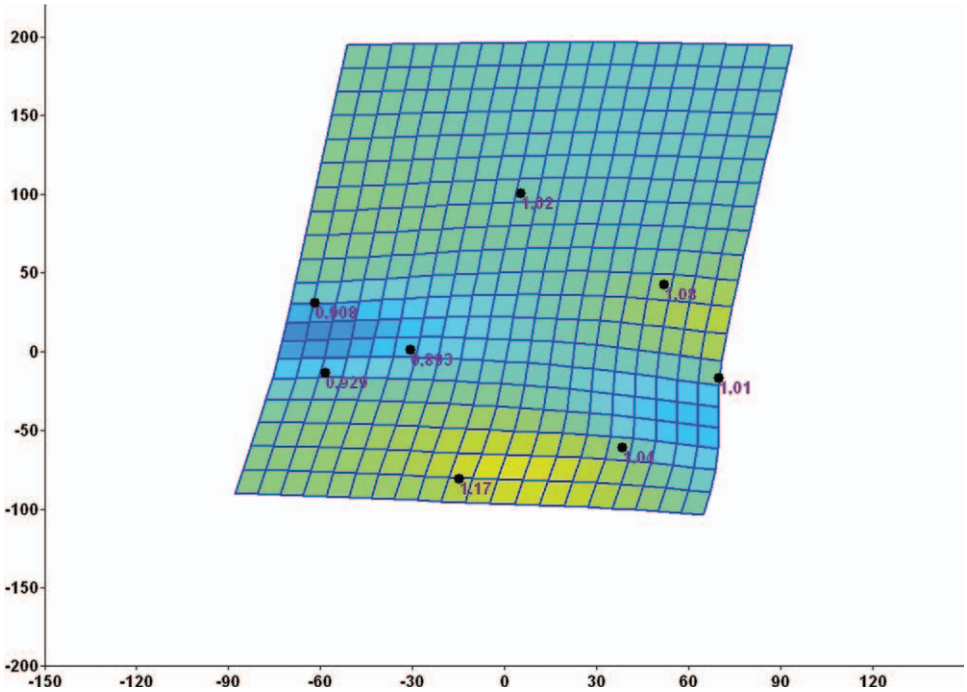

Fig. 10. A thin-plate spline demonstrating the average cerebellum shape deformation from controls to secondary progressive MS patients.

analysis method (He et al., 2007; Ishaq et al., 2007; Shuyu et al., 2007; Çolak et al., 2011). Shuyu et al. (2007) reported that the CC of Alzheimer's disease appeared globally atrophic, but the atrophy in the posterior part was more evident than the other parts. Also, the authors concluded that the lower edge showed more extension than the upper edge of the CC. In another study, investigating CC in autism (He et al., 2007), a significant difference was found between patients and controls in the body of the CC. Ishaq et al. (2007) have performed a medial-based global and regional statistical analysis of the CC shape in MS, and showed that the effect of the deformations on the shape variation was significantly different for the various CC subdivisions. Among the reasons for the differences in the pattern of regional distribution of CC damage, a variable amount of thin fibers in the different regions of this structure should be considered because thin fibers are more vulnerable to MS-related injury (Evangelou et al, 2001). In this study, we found maximum deformation to be located in the anterior region (genu and rostrum) of the CC from controls to RRMS. In SPMS, maximum deformations were found in the anterior region of CC (genu and rostrum) and truncus. In a study, calculating the densities of fibers of different sizes in different regions of the CC, it was found that thin fibers were most dense in the anterior CC (genu) and decreased in density toward the posterior midbody, where they reached a minimum (Aboitiz et al., 1992). These findings are in line with our results, and can be the reason of the high deformation, which we found in the anterior region of the CC. The deformations found in the anterior region in RRMS group, to become even more prominent in the SPMS group and extend to the region of truncus, can be considered as an expected result of the progressive nature of SPMS.

Also, we studied the cerebellum because neuropathological observations have indicated that the cerebellar cortex is a major site of demyelination in different MS forms (Kutzelnigg et al., 2007). In recent years, several studies have suggested that the cerebellar cortex may be a central locus of tissue damage in MS using different methods (Anderson, 2009; Calabrese, 2010). Cerebellum has been identified as a region of gray matter loss in voxel-based morphometry studies of patients with progressive MS. Lin et al. (2003) found a significant difference in whole cerebellar volume between patients with SPMS and controls, but not between RRMS patients and controls. Anderson et al. (2009) has also observed more explicit atrophy in SPMS compared with RRMS patients and have reported that this atrophy is associated with progressive disability. Moreover, Ramasamy et al. (2009) has found significant volume loss in the cerebellar WM when comparing MS patients and clinically isolated syndrome patients with healthy controls, by using logistic regression and linear model analytical methods. We also investigated the shape deformation of cerebellum in the different clinical phenotypes of MS using statistical shape analysis method and found significant differences between the cerebellar shapes of SPMS patients and controls, and relatively less significant differences between the cerebellar shapes of RRMS patients and controls. The enhanced significance found in the SPMS group supports previous findings in the literature (Lin et al., 2003; Anderson et al., 2009). Cerebellar shape deformation from controls to SPMS patients was greater than the

deformation from controls to RRMS patients. In relapsing-remitting, group maximum deformations were particularly localized in the posterior lobe of the cerebellum. Furthermore, limited deformations were found in the anterior lobe of the cerebellum. In the secondary progressive group, maximum deformations were identified in the anterior lobe and fewer deformations were found in the posteroinferior lobe of the cerebellum. Stoodley and Schmahmann (2010) found converging lines of evidences supporting regional organization of motor, cognitive, and limbic behaviors in the cerebellum, and presented a functional topography for the cerebellum. They reported that the lesions affecting anterior lobe and lobule VI of the cerebellum lead to motor dysfunctions, whereas the lesions in the posterior lobe affecting lobule VI and VII lead to cognitive impairment (Stoodley and Schmahmann, 2010). With the aforementioned functional topographical data, our study results showed the more prominent involvement of the motor system and cognition in SPMS and RRMS, respectively. This is also an expected finding because as a MS patient progresses from RRMS to SPMS, motor system involvement became more pronounced. Also, deformation found in the anterior lobe in SPMS patients being more than the one in RRMS, can be thought as the indicator that, motor dysfunction, compared with cognition, is more prominently affected in SPMS than RRMS.

The infratentorial lesion is one of many factors that affect the prognosis of MS patients. The comparison of the cerebellum and CC shapes of all of the MS patients in this study, irrespective of their classification of RRMS or SPMS, according to presence of an infratentorial lesion, showed that there were no significant differences observed between these two groups in terms of cerebellar and CC shapes.

In conclusion, this study showed that shape deformations in the CC and cerebellum are present in MS patients. Statistical shape analysis, demonstrated selective CC and cerebellum damage, even if more pronounced in SPMS, in both patient groups. This is the first study to show that both CC and cerebellar shape differences in MS patients can be evaluated using a landmark-based geometrical morphometric method, by taking into consideration the topographic distribution of CC and cerebellum. We hope that the results obtained from this study serve as a reference for future clinical studies.

LITERATURE CITED

Aboitiz F, Scheibel AB, Fisher RS, Zaidel E. 1992. Fiber composition of the human corpus callosum. Brain Res 598:143–153.

Anderson VM, Fisniku LK, Altmann DR, Thompson AJ, Miller DH. 2009. MRI measures show significant cerebellar gray matter volume loss in multiple sclerosis and a reassociated with cerebellar dysfunction. Mult Scler 15:811–817.

Bookstein FL. 1991. Morphometrics tools for landmark data. New York: Cambridge University Press.

Calabrese M, Mattisi I, Rinaldi F, Favaretto A, Atzori M, Bernardi V, Barachino L, Romualdi C, Rinaldi L, Perini P, Gallo P. 2010. Magnetic resonance evidence of cerebellar cortical pathology in multiple sclerosis. J Neurol Neurosurg Psychiatry 81:401–404.

Ceccarelli A, Rocca MA, Pagani E, Colombo B, Martinelli V, Comi G, Filippi M. 2008. A voxel-based morphometry study of grey matter loss in MS patients with different clinical phenotypes. Neuroimage 42:315–322.

Colak C, Ercan I, Dogan M, Ozdemir ST, Sener S, Alkan A. 2011. Detecting the shape differences of the corpus callosum in Behçet's disease by statistical shape analysis. Anat Rec 294:870–874.

Compston A, Coles A. 2008. Multiple sclerosis. Lancet 372: 1502–1517.

Confavreux C, Vukusic S. 2006. Age at disability milestones in multiple sclerosis. Brain 129:595–605.

DeQuardo JR, Keshavan MS, Bookstein FL, Bagwell WW, Green WD, Sweeney JA, Haas GL, Tandon R, Schooler NR, Pettegrew JW. 1999. Landmark-based morphometric analysis of first-episode schizophrenia. Biol Psychiatry 45:1321–1328.

Dimitrov DM. 2006. Reliability. In: Erford BT, editor. Assessment for counselors. Boston: Houghton-Mifflin/Lahaska Press. Chapter 3, p 99–122.

Dryden IL, Mardia KV. 1998. Statistical shape analysis. New York: Wiley.

Dryden IL. 2009. Shapes: statistical shape analysis. R package version 1.1–3. Available at: http://cran.r-project.org/.

Ercan I, Ocakoglu G, Guney I, Yazici B. 2008. Adaptation of generalizability theory for inter-rater reliability for landmark localization. Int J Tomogr Stat 9:51–58.

Ercan I, Ocakoglu G, Sigirli D, Ozkaya G. 2012. Statistical shape analysis and usage in medical sciences. Turkiye Klinikleri J Biostat 4, 27–35.

Evangelou N, Konz D, Esiri MM, Smith S, Palace J, Matthews PM. 2001. Size-selective neuronal changes in the anterior optic pathways suggest a differential susceptibility to injury in multiple sclerosis. Brain 124:1813–1820.

Hammer Ø, Harper DAT, Ryan PD. 2001. PAST: Paleontological statistics software package for education and data analysis. Palaeontologia Electronica 4:9.

He Q, Duan Y, Miles JH, Takahashi TN. 2007. Statistical shape analysis of the corpus callosum in subtypes of autism. In: IEEE 7th International Symposium on Bioinformatics and Bioengineering, Boston, Massachusetts, Oct 14–17, 2007.

Hines M, Chiu L, McAdams LA, Bentler PM, Lipcamon J. 1992. Cognition and the corpus callosum: verbal fluency, visuospatial ability, and language lateralization related to midsagittal surface areas of callosal subregions. Behav Neurosci 106:3–14.

Ishaq O, Hamarneh G, Tam R, Traboulsee A. 2007. Longitudinal, regional and deformation-specific corpus callosum shape analysis for multiple sclerosis. Conf Proc IEEE Eng Med Biol Soc 2110–2113. DOI: 10.1109/IEMBS.2007.4352738.

Kutzelnigg A, Faber-Rod JC, Bauer J, Lucchinetti CF, Sorensen PS, Laursen H, Stadelmann C, Brück W, Rauschka H, Schmidbauer M, Lassmann H. 2007. Widespread demyelination in the cerebellar cortex in multiple sclerosis. Brain Pathol 17:38–44.

Lin X, Blumhardt LD, Constantinescu CS. 2003. The relationship of brain and cervical cord volume to disability in clinical subtypes of multiple sclerosis: a threedimensional MRI study. Acta Neurol Scand 108:401–406.

McDonald WI, Compston A, Edan G, Goodkin D, Hartung HP, Lublin FD, McFarland HF, Paty DW, Polman CH, Reingold SC, Sandberg-Wollheim M, Sibley W, Thompson A, Van Den Noort S, Weinshenker BY, Wolinsky JS. 2001. Recommended diagnostic criteria for multiple sclerosis: guidelines from the International Panel on the diagnosis of multiple sclerosis. Ann Neurol 50: 121–127.

Morgen K, Sammer G, Courtney SM, Wolters T, Melchior H, Blecker CR, Oschmann P, Kaps M, Vaitl D. 2006. Evidence for a direct association between cortical atrophy and cognitive impairment in relapsing-remitting MS. Neuroimage 15:891–898.

Ozdemir ST, Ercan I, Sevinc O, Guney I, Ocakoglu G, Aslan E, Barut C. 2007. Statistical shape analysis of differences in the shape of the corpus callosum between genders. Anat Rec 290: 825–830.

Quarantelli M, Ciarmiello A, Morra VB, Orefice G, Larobina M, Lanzillo R, Schiavone V, Salvatore E, Alfano B, Brunetti A. 2003. Brain tissue volume changes in relapsing-remitting multiple sclerosis: correlation with lesion load. Neuroimage 18:360–366.

Pierson R, Corson PW, Sears LL, Alicata D, Magnotta V, Oleary D, Andreasen NC. 2002. Manual and Semiautomated Measurement of Cerebellar Sub regions on MR Images. Neuroimage 17: 61–76.

Ramasamy DP, Benedict RH, Cox JL, Fritz D, Abdelrahman N, Hussein S, Minagar A, Dwyer MG, Zivadinov R. 2009. Extent of cerebellum, subcortical and cortical atrophy in patients with MS: a case-control study. J Neurol Sci 282: 47–5.

Reynolds R, Roncaroli F, Nicholas R, Radotra B, Gveric D, Howell O. 2011. The neuropathological basis of clinical progression in multiple sclerosis. Acta Neuropathol 122:155–170.

Rohlf FJ. 2010. TPSDIG Version 2.16. Ecology and Evaluation, SUNY at Stony Brook, New York.

Shuyu L, Fang P, Xiangqi H, Li D, Tianzi J. 2007. Shape analysis of the corpus callosum in alzheimer's disease. Bioinformatics and Biomedical Engineering ICBBE 2007; The 1st International Conference; p. 1095–1098. (doi: 10.1109/ICBBE. 2007.283).

Sibony P, Kupersmith MJ, Rohlf FJ. 2011. Shape analysis of the peripapillary RPE layer in papilledema and ischemic optic neuropathy. Invest Ophthalmol Vis Sci 52:7987–7995.

Sonat F, Ercan I, Ozdemir ST, Ozkaya G, Noyan B. 2009. Statistical shape analysis of the rat hippocampus in epilepsy. Anat Sci Int 84:298–304.

Stoodley CJ, Schmahmann JD. Evidence for topographic organization in the cerebellum of motor control versus cognitive and affective processing. 2010. Cortex 46:831–844.

Styner M, Lieberman JA, Pantazis D, Gerig G. Boundary and medial shape analysis of the hippocampus in schizophrenia. 2004. Med Image Anal 8:197–203.

Tibbo P, Nopoulos P, Arndt S, Andreasen NC. 1998. Corpus callosum shape and size in male patients with schizophrenia. Biol Psychiatry 44:405–412.

Wan J, Shen L, Fang S, McLaughlin J, Autti-Rämö I, Fagerlund A, Riley E, Hoyme HE, Moore ES, Foroud T. A framework for 3D analysis of facial morphology in fetal alcohol syndrome. 2010. Lect Notes Comput Sci 6326:118–127.

Weinberg SM, Andreasen NC, Nopoulos P. 2009. Three-dimensional morphometric analysis of brain shape in nonsyndromic orofacial clefting. J Anat 214, 926–936.

Weisbecker V. 2012. Distortion in formalin-fixed brains: using geometric morphometrics to quantify the worst-case scenario in mice. Brain Struct Funct 217:677–678.